

Original Article

Fractional Order Internal Mode Control Proportional Integral Derivative (FOIMCPID) Controller Fed Design for Depth Control of Autonomous Underwater Vehicle

Linkan Priyadarsini¹, Shubhasri Kundu², Manoj Kumar Maharana³

^{1,2,3}School of Electrical Engineering, KIIT Deemed to be University, Odisha, India.

¹Corresponding Author : linkanpriyadarsini88@gmail.com

Received: 17 September 2023

Revised: 19 October 2023

Accepted: 15 November 2023

Published: 30 November 2023

Abstract - Autonomous Underwater Vehicles (AUVs) can replace humans in dangerous situations and have many applications due to their endurance, stealthiness, intelligence, and versatility. Many studies have focused on developing better motion control systems for AUVs so that the vehicles can remain steady despite the waves. The present research focuses on developing a controller for regulating the depth of an Autonomous Underwater Vehicle (AUV). The proposed controller uses the Fractional Order-based Internal Mode Control Proportional Integral Derivative (FOIMCPID) technique. In this research, we suggest implementing a Fractional-Order Proportional Integer Derivative (FOPID) controller into an AUV motion control system. It improves the standard PID controller by boosting the value of two tuning parameters. This study uses Internal Model Control (IMC) to tune the Fractional Order Controllers class. This tuning rule was developed without using any time delay approximations. A similar-tuned industrial PID controller and FOPID are compared to demonstrate the value of fractional order controllers compared to traditional integer order controllers. After that, the robust stability of both controllers is examined in controlling the heading angle of Autonomous Underwater Vehicles (AUVs).

Keywords - AUV, FOPID, IMC, FOIMCPID, Controller, Fractional Order.

1. Introduction

The arrival of self-driving cars is just one example of how modern technology has changed the world. Over the past few decades, there have been two primary schools of thought when studying underwater jobs. Firstly, techs run the equipment and talk to people on the surface through divers. In the second way, the technician must be at the water's surface for the equipment to work [1]. These techniques are effective but inconvenient since they place men in risky positions and waste agents.

AUV technology is used in many different fields, like oil and gas, marine biology, and the military, to name a few. AUV have been looked into many times to try to solve different technology problems. Both internal and outside forces, like a vital water current or too much pressure on the body, could threaten the Autonomous Underwater Vehicle (AUV). The generalization of integration and differentiation to any order is represented by fractional calculus. The interest in generalizing classical control theories and creating cutting-edge fractional calculus-based control techniques is rising. The PID controller, a particular instance of fractional order $PI\mu D\lambda$, is the most widely used technique for managing a wide range of operations.

Numerous researchers have demonstrated a keen interest in the design intricacies of fractional order controllers. Their scholarly contributions have yielded commendable outcomes, showcasing the utilization of fractional order controllers across diverse processes to enhance control systems' performance and robustness. Due to the additional tuning variables, μ and λ , fractional order PID controllers are chosen based on their ability to enhance control performance.

The fractional controller can complete more specifications since it has more parameters than a traditional controller, which improves system performance overall and increases the system's resistance to modelling uncertainties. Because of the design's simplicity and foundation in inverting the process model, the Internal Model Control (IMC) [2] based PID controller has achieved significant recognition in the control field. A proposed method for fracting fractional order $PI\mu D\lambda$ based on a firefly algorithm [3].

The primary goal of this research is to improve the depth stability of Autonomous Underwater Vehicle (AUV) dynamics in the presence of disturbances by developing a controller scheme called a Fractional Order -based Internal Model Control Proportional Integral Derivative controller



(FOIMCPID). The coefficients of the FOIMCPID controller were designed utilizing the FFA method to boost the AUV's performance and transient responsiveness. Maintaining system stability in the face of uncertainty, such as the presence of underwater currents, is a crucial indicator of the performance of the suggested controller [4].

The organizational framework of the article can be delineated as follows: Section 2 provides an overview of the modeling strategy employed for the Autonomous Underwater Vehicle (AUV), while Section 3 delves into the formulation and advancement of the suggested control methodology. The following section presents simulation results demonstrating the proposed technique's efficacy in the Autonomous Underwater Vehicle (AUV) diving and steering motions. Section 5 presents a concise summary of the findings.

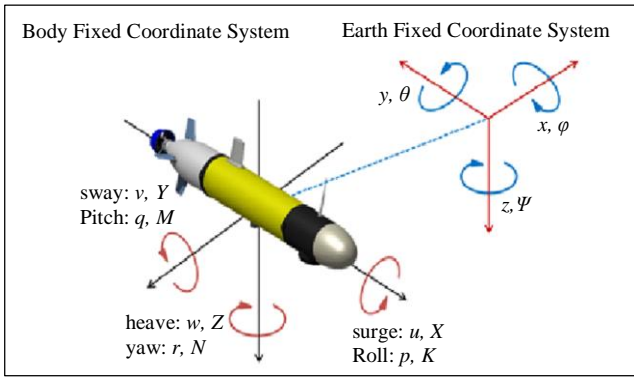


Fig. 1 Prototype of AUV

2. Modelling of Autonomous Underwater Vehicles

Six degrees of freedom are necessary to adequately characterize the vehicle's location and orientation to investigate the movement of marine vehicles. The initial three sets of coordinates and their respective time derivatives are necessary to describe position and translation motion. The last three sets of coordinates and corresponding time derivatives are required for orientation and rotational motion.

Table 1. Parameters of AUV

Variable Quantity	Motion	Potency and Moments	Velocity	Position and Euler Angles
A	Surge	X	u	x
B	Sway	Y	v	y
C	Heave	Z	w	z
D	Roll	K	P	ϕ
E	Pitch	M	q	θ
F	Yaw	N	r	ψ

To obtain a mathematical model of the Autonomous Underwater Vehicle (AUV), the examination of its performance can be divided into two independent domains: kinematics and dynamics. Kinematics is the branch of physics concerned with analysing objects either stationary or moving at a constant velocity. On the other hand, dynamics is the field of study that examines things that undergo accelerated motion.

2.1. Vehicle Kinematics

Two coordinate frames are chosen to analyze 6 Degrees of Freedom (DOF) vehicle motion. The body-fixed reference frame, or moving reference frame, is permanently fixed to the vehicle. The utilization of the notion of an inertial frame serves to delineate the motion of a frame that remains stationary relative to an object. The consideration of acceleration experienced by a point on the Earth's surface is commonly overlooked in discussions about maritime vehicles. Due to this circumstance, considering the Earth's fixed frame as an inertial one is plausible. This suggests that it is necessary to establish the position and alignment of the vehicle to a non-accelerating reference frame, known as an inertial frame. Additionally, the vehicle's linear and rotational motion rates should be described using a frame of reference fixed to the car itself, referred to as a body-fixed frame.

$$\eta = \begin{bmatrix} \eta_1 \\ \eta_2 \end{bmatrix}$$

$$\eta_1 = \begin{bmatrix} x \\ y \\ z \end{bmatrix} \text{ Position vector}$$

$$\eta_2 = \begin{bmatrix} \phi \\ \theta \\ \psi \end{bmatrix} \text{ Euler angles vector}$$

$$v = \begin{bmatrix} v_1 \\ v_2 \end{bmatrix}$$

$$v_1 = \begin{bmatrix} u \\ v \\ w \end{bmatrix} \text{ Uniform speed vector}$$

$$v_2 = \begin{bmatrix} p \\ q \\ r \end{bmatrix} \text{ Rotational speed vector}$$

$$\tau = \begin{bmatrix} \tau_1 \\ \tau_2 \end{bmatrix}$$

$$\tau_1 = \begin{bmatrix} X \\ Y \\ Z \end{bmatrix} \text{ Forces direction}$$

$$\tau_2 = \begin{bmatrix} K \\ M \\ N \end{bmatrix} \text{ Moments vector}$$

2.2. Vehicle Dynamics

The vehicle's dynamics encompass both linear and rotary motion.

$$m(v_0 + \omega * r_g + \omega * (\omega * r_g)) = f_0 \quad (1)$$

The rotational movement of the vehicle is as follows:

$$I_0 \omega + \omega * (I_0 \omega) + m r_g \dot{v}_0 = m_0 \quad (2)$$

With the help of Newton-Euler's equation, the 6 DOF equation of an AUV can be written as,

$$m(u - vr + wp - x_g(q^2 + r^2) + y_g(pq - \dot{r}) + z_g(pr + \dot{q})) = X \quad (3)$$

$$m(v - wp + ur - y_g(\dot{r}^2 + p^2) + z(qr - \dot{p}) + x_g(qp + \dot{r})) = Y \quad (4)$$

$$m(w - uq + vp - z_g(p^2 + q^2) + x_g(rp - \dot{q}) + y_g(rq + \dot{p})) = Z \quad (5)$$

$$I_x \dot{p} + (I_z - I_y)qr - (\dot{r} + pq)I_{xz} + (r^2 - q^2)I_{yz} + (pr - \dot{q})I_{xy} + m[y_g(\dot{w} - uq + vq) - z_g(\dot{v} - wp + wr)] = K \quad (6)$$

$$I_y \dot{q} + (I_x - I_z)rp - (\dot{p} + qr)I_{xy} + (p^2 - r^2)I_{xz} + (qp - \dot{r})I_{yz} + m[z_g(\dot{u} - vr + wq) - x_g(\dot{w} - uq + vp)] = M \quad (7)$$

$$I_z \dot{r} + (I_y - I_x)pq - (\dot{q} + rp)I_{yz} + (q^2 - p^2)I_{xy} + (rq - \dot{p})I_{xz} + m[x_g(\dot{v} - wp + ur) - y_g(\dot{u} - vr + wq)] = N \quad (8)$$

The kinematics for AUV pitch and depth subsystem by linearizing the kinematics and dynamics of AUV and neglecting the terms not required for modelling the subsystem is given by:

$$x = \cos(\theta u) + \sin(\theta w) \quad (9)$$

$$z = -\sin(\theta u) + \sin(\theta w)$$

$$\theta = q$$

With the help of the Maclaurin series of trigonometric terms, the linearized equation obtained after neglecting the higher order terms we get,

$$x = u + \theta w \quad (10)$$

$$z = -u_1 \theta + w \quad (11)$$

$$\Theta = q \quad (12)$$

Similarly, the dynamic equations are given by,

$$m(u + wq - x_g q^2 + z_g q) = X \quad (13)$$

$$m(w - uq - z_g q^2 + x_g q) = Z \quad (14)$$

$$I_y q + m[z_g(u + wq) + x_g(w - uq)] = M \quad (15)$$

Linearizing the above equation, we get

$$m(u + z_g q) = X \quad (16)$$

$$m(w - x_g q - u_1 q) = Z \quad (17)$$

$$I_y q + m[z_g(u - x_g(w - u_1 q))] = M \quad (18)$$

Under the premise that the heave speed is negligible and can be disregarded, the motion and dynamics of the vehicle can be expressed in matrix form:

$$\begin{bmatrix} I_y - M_q & 0 & 0 \\ 0 & 1 & 0 \\ 0 & 0 & 1 \end{bmatrix} \begin{bmatrix} q \\ z \\ \theta \end{bmatrix} + \begin{bmatrix} -M_q & 0 & M_\theta \\ 0 & 0 & u_1 \\ -1 & 0 & 0 \end{bmatrix} \begin{bmatrix} q \\ z \\ \theta \end{bmatrix} = \begin{bmatrix} M_{fs} \\ 0 \\ 0 \end{bmatrix} \quad (19)$$

The pitch transfer function obtained from the above matrix is given by,

$$G_\theta(s) = \frac{\theta(s)}{f_s(s)} = \frac{\frac{M_{fs}}{I_y - M_q}}{s^2 - \frac{M_{fs}}{I_y - M_q} - \frac{M_\theta}{I_y - M_q}} \quad (20)$$

Considering the input pitch angle, the depth can be represented by the following transfer function:

$$G_z(s) = \frac{z(s)}{\theta(s)} = \frac{-u_1}{s} \quad (21)$$

Using the following information, we can figure out the transfer function for the AUV:

Table 2. Parametric values

Parameter	Value
Fin Lift (M_{fs})	-1575.9 kg.m2/s
I_y	469 kg/m2
Added Mass (M_q)	-458 kg.m2
Hydrostatic (M_θ)	13719.6 kg.m2/s2

$$G_\theta(s) = \frac{3.18}{s^2 + 1.09s + 0.52} \quad (22)$$

Assuming a linear velocity of 11 m/s, the transfer function of depth is given by

$$G_z(s) = \frac{11}{s} \quad (23)$$

3. Controller Design

Here, we will examine the controller design considerations required to achieve AUV system stability. We use FOPID, IMCPID and FOIMC-PID to control the yaw angle. The control design succeeds if the system's paths reach the surface within time.

3.1. Internal Mode PID (IMCPID) Controller [10]

The Proportional-Integral-Derivative (PID) controller is widely used in manufacturing and other commercial establishments. Its primary purpose is to boost performance in linear systems; hence, its utility in nonlinear contexts is restricted. An IMC-based Proportional-Integral-Derivative (PID) controller has been created to overcome the limitations of conventional PID controllers. Implementing the IMC-PID controller has been seen to boost the ability to track set points and enhance the rejection of disturbances in systems with higher orders [2]. The transfer function of a controller symbolised as $Q(s)$, is a mathematical expression employed to elucidate the correlation between the input and output of a controller system.

$$q(s) = \frac{G_c(s)}{1+G_M(s)G_c(s)} \tag{24}$$

$$G_c(s) = \frac{q(s)}{1-G_M(s)q(s)} \tag{25}$$

Where, $G_M(s) = G_M^+(s)G_M^-(s)$ (26)

$$q(s) = (G_M^+(s))^{-1}F(s) \tag{27}$$

Where, $F(s) = \frac{1}{(1+s)^{m'}}$ (28)

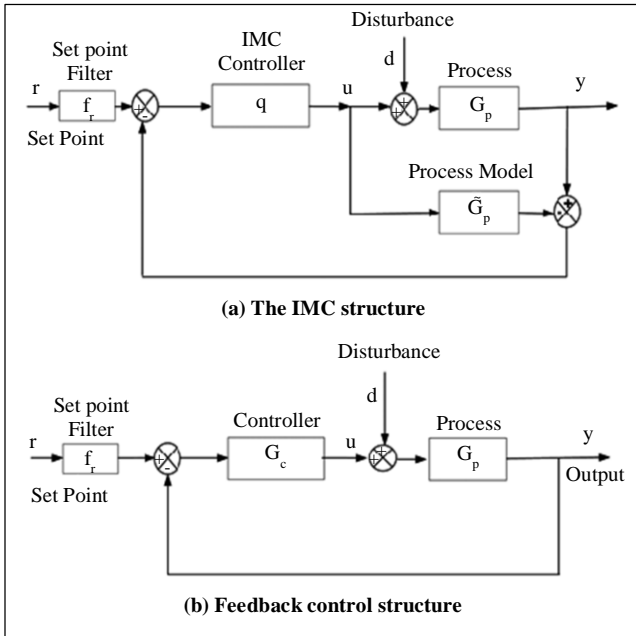


Fig. 2 IMC-PID controller

$G_M^-(s)$ is the model of the system outside of its minimal phase. The symbol η denotes the tuning parameter, also known as a closed-loop system's filter constant or time constant. η describes how quickly the system can react, while m is a positive integer above which $Q(s)$ becomes practically achievable.

The fractional order PID can be mathematically represented in the following form:

$$C(s) = k_p + \frac{k_i}{s^\lambda} + k_d s^\mu \tag{29}$$

3.2. Fractional Order PID (FOPID) [8, 11]

The Fractional order PID controller can be described as

$$G_{PID}(s) = k_p + \frac{k_i}{s^\lambda} + k_d s^\mu \tag{30}$$

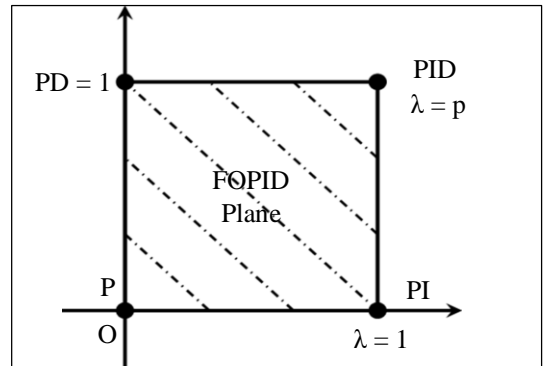


Fig. 3 XY plane

Where λ and μ are fractional numbers. The present study aims to develop a mathematical model for a fractional algorithm. The PID controller consists of five tunable parameters, namely $k_p, k_i, k_d, \lambda,$ and μ . The values of λ and μ are rational numbers that fall from 0 to 1. The Fractional Order Proportional-Integral-Derivative (FOPID) controller exhibits characteristics similar to a standard PID controller when the values of λ and μ are set to 1. The Firefly Algorithm (FFA) optimised the Fractional Order Proportional Integral Derivative (FOPID) controller.

3.3. Firefly Algorithm [3]

After Krishnanad talked about it in 2005 [6], Dr. Xin She Yang developed the Firefly algorithm. It is a meta-heuristic optimisation method based on how things work in nature. This optimisation method has been changed to match how fireflies behave and how they flash. This programme is founded around three fundamental principles:

- Fireflies exhibiting the most intense luminosity are attracted to other fireflies demonstrating similar behaviour, forming cohesive groups. This phenomenon holds for fireflies of both genders, irrespective of their sex.

- The light of the fireflies is what draws people to them. The group will be brighter when the fireflies are close to each other. If there are no stronger fireflies, they will move around randomly.
- The brightness or attractiveness of the fireflies will depend on the objective function that is picked.

The firefly's allure is determined by -

$$\beta = \beta_0 e^{-\gamma r^2} \quad (31)$$

The variable "r" represents the distance between firefly i and firefly j, with firefly i located at position X_i and firefly j at position X_j .

The first answer can be written as

$$X_j = rand(Ub - Lb) + Lb \quad (32)$$

Based on the above equation, firefly I is attracted to firefly j, which possesses a higher luminosity.

$$X_i^{r+1} = X_i^r + \beta e^{-\gamma r_{ij}^2} + \alpha_t(rand - \frac{1}{2}) \quad (33)$$

The first steps of the Firefly Algorithm are to define the Objective Function and create a random starting population. Then, the optimisation parameters are specified. The Integral of Absolute Error (IAE) was chosen as the objective function for the FA Algorithm., which is mathematically defined as follows:

$$IAE = \int_0^{\infty} |e(t)| dt \quad (34)$$

3.4. Fractional Order IMC based PID (FO-IMC-PID) [6]

The system model is created by the linearization process described as,

$$G(s) = \frac{3.18}{s^2 + 1.09s + 0.52} \quad (35)$$

As seen in Section 3, the model $G_m(s)$ can be factorized as,

$$G_M^-(s) = \frac{3.18}{s^2 + 1.09s + 0.52}; G_M^+(s) = 1 \quad (36)$$

In expression (36), the symbol $G_M^-(s)$ stands for the minimum phase component, and the symbol $G_M^+(s)$ stands for the original system model $G(s)$'s non-minimum phase component.

After factorization, a filter is chosen, as shown in eqn (37). Here, the factor is set by what makes sense. Here, the most important thing to do is pick the factor m. Here, m is set to 1. The IMC processor was made in such a way that:

$$Q(s) = \frac{1}{G_m(s)} f(s) \quad (37)$$

$$Q(s) = \frac{s^2 + 1.09s + 0.52}{3.18} \frac{1}{(1 + \eta s)} \quad (38)$$

The usual feedback controller form is shown in Equation (2). This is done by rearranging the Equation (38) that shows the Internal Model controller.

$$C(s) = \frac{s^2 + 1.09s + 0.52}{3.18(\eta s)}; \eta = 0.1 \quad (39)$$

$$C(s) = \frac{1.09}{3.18\eta} + \left(\frac{0.52}{3.18\eta}\right)\frac{1}{s} + \frac{1}{3.18\eta} s \quad (40)$$

$$\text{i.e., } k_p = \frac{1.09}{3.18\eta}, k_i = \frac{0.52}{3.18\eta}, k_d = \frac{1}{3.18\eta}$$

$$C(s) = 3.42 + \frac{1.635}{s} + 3.144s \quad (41)$$

Furthermore, the values of λ and μ are established by applying a trial-and-error methodology. In this specific case, the values that have been obtained are,

$$\lambda = 3.05 \text{ and } \mu = 1.81$$

Hence, the Fractional Order IMC based PID controller is given by,

$$C_{FOIMCPID}(s) = 3.42 + \frac{1.635}{s^{3.05}} + 3.144s^{1.81} \quad (42)$$

4. Performance Analysis

Fractional Order PID (FO-PID) and conventional IMC (IMCPID) controllers are examined and contrasted with the suggested Fractional Order IMC-PID (FO-IMC-PID) controller. Time-to-reject disturbances and integral error criteria, such as Integral Absolute Error (IAE), are used in the assessment. In this case, after 10 seconds, a 0.1-magnitude step disruption is introduced to the system. This study encompassed the execution of two simulation trials to assess the robustness and efficacy of the suggested heading control system.

4.1. Depth Control Devoid of Agitating Forces

The reaction of the depth angle with the IMC-PID, FOPID and FOIMCPID controllers applied for a desired depth is depicted in Figures 4 and 5. The findings suggest that the FOIMCPID controller exhibits enhanced performance compared to the IMCPID and FOPID controller. These characteristics are seen in the system's enhanced temporal response, decreased settling time, minimised overshoot, and increased damping. Table 3 displays a comparative analysis of the transient responsiveness of the controllers. The superiority of the fractional controller's performance is apparent across all characteristics.

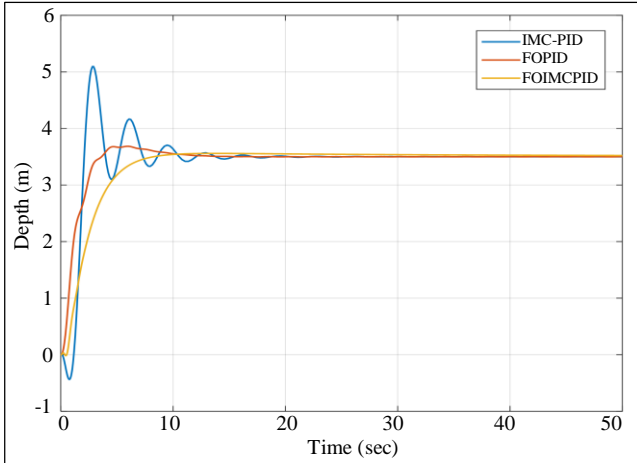


Fig. 4 Depth response in the absence of disturbance

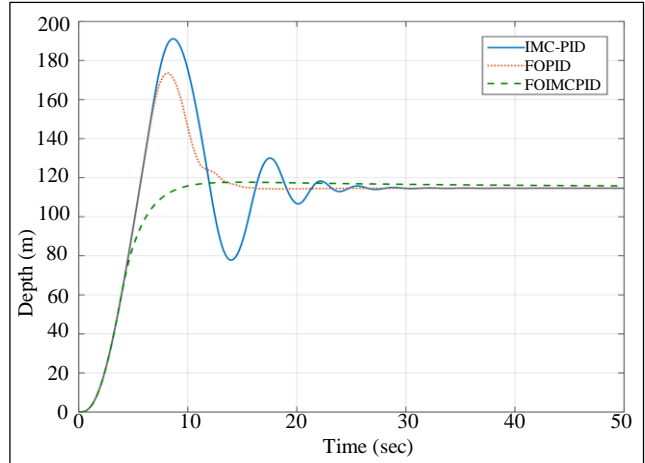


Fig. 6 Depth response in the presence of disturbance

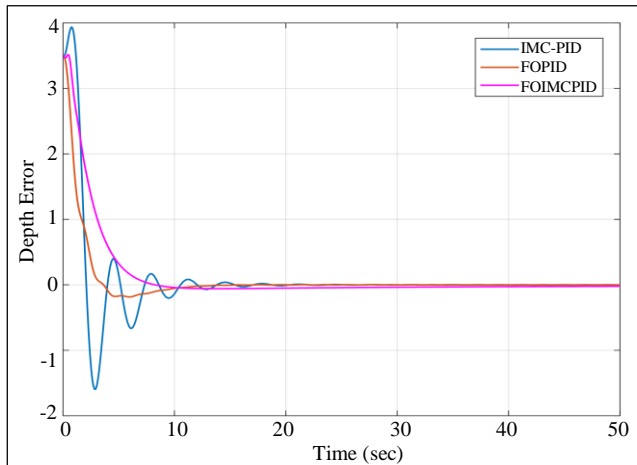


Fig. 5 Depth error in the absence of disturbance

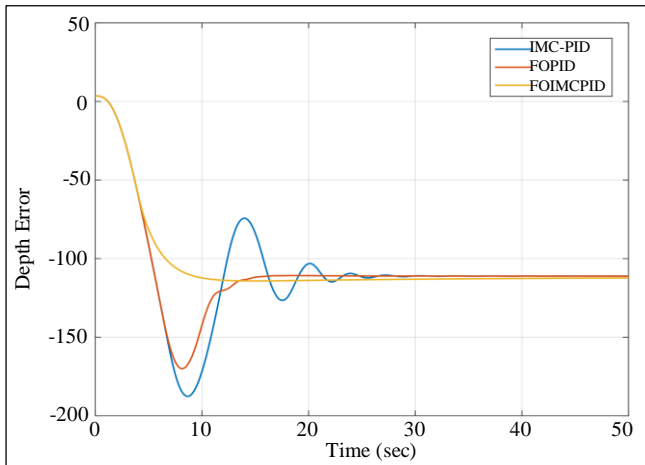


Fig. 7 Depth error in the presence of disturbance

Table 3. Depth response without disturbing forces

Response	Controller		
	IMC-PID	FOPID	FOIMCPID
Rise Time	1.07	0.89	0.56
Settling Time	8.87	5.37	4.75
Overshoot	7.19	6.8	4.69
Peak Time	2.21	0.99	0.591
IAE	8.573	7.798	6.897

Table 4. Depth response with disturbances

Response	Controller		
	IMC-PID	FOPID	FOIMCPID
Rise Time	1.04	1	0.94
Settling Time	10.77	8.76	5.83
Overshoot	9.3	7.36	6.83
Peak Time	11.56	10.6	1.81
IAE	21.42	20.34	18.97

4.2. Analysing the AUV's Depth Control in the Face of Disturbance

Figures 6 and 7 depicts the reaction of the depth in the presence of an external disturbance, namely ocean current waves, exerting influence on the Autonomous Underwater Vehicle (AUV) system. The FOIMCPID controller demonstrates superior performance compared to the IMC-PID and FOPID controller in terms of time response, overshoot, and settling time for achieving the target depth in the presence of external disturbances.

Table 4 presents a comparison of the reactions among the controllers. The implementation of the fractional order-based IMC PID controller resulted in an enhancement of the transient responsiveness across all dimensions.

4.3. Estimating the AUV's Depth Control in Noise Conditions

The response of Autonomous Underwater Vehicle (AUV) vertical movement is subject to distortion due to evolving additive white noise.

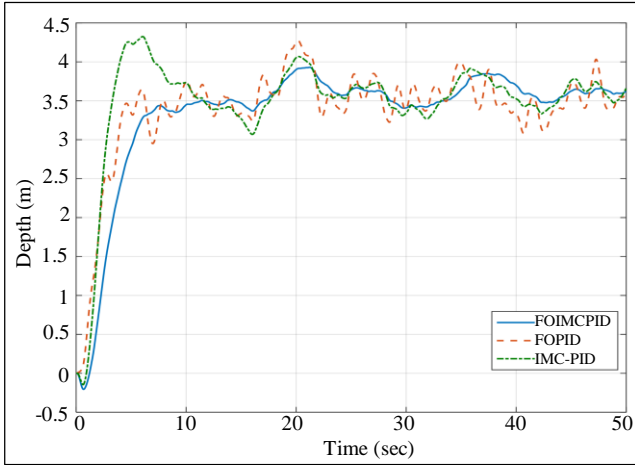


Fig. 8 Depth response in the presence of noise

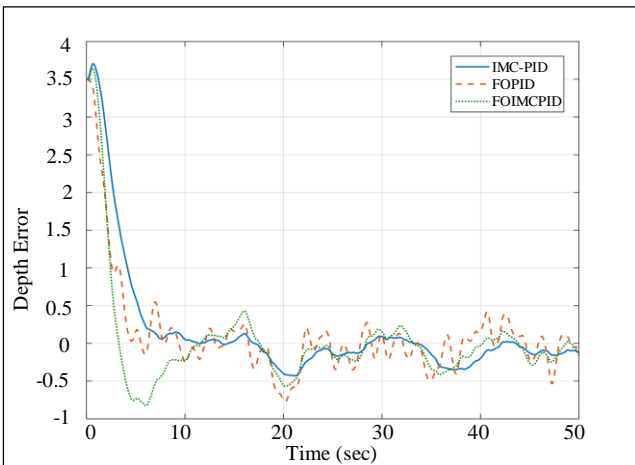


Fig. 9 Depth error in the presence of noise

Table 5. Depth response with noise

Response	Controller		
	IMC-PID	FOPID	FOIMCPID
Rise Time	1.24	1.07	0.998
Settling Time	5.93	5.89	5.36
Overshoot	0.369	0.269	0
Peak Time	7.11	3.98	1.69
IAE	16.76	15.56	13.83

Figures 8 and 9 displays IMCPID, FOPID, and the FOIMCPID response based on the FFA algorithms, with an increased noise power of 0.001. Table 5 presents the outcomes for each curve in terms of time specifications, such as rising time, settling time, and maximum peak overshoot, when the noise power of 0.001 is employed.

5. Conclusion

The AUV model is constructed using linearized vertical motion control. However, noise originating from sensors or low turbulence on the AUV has resulted in distortions in the response settling time and overshoot. Various control methods, such as Internal Mode Control PID (IMC-PID), Fractional Order PID (FOPID) and Fractional Order based Internal Model Control PID (FOIMCPID), were employed in this study. These control schemes were tuned using a Firefly Algorithm (FFA).

Acknowledgments

An acknowledgment to the School of Electrical Engineering, KIIT, Deemed to be University, Bhubaneswar, Odisha, India.

References

- [1] V. Upadhyay et al., "Design and Motion Control of Autonomous Underwater Vehicle, Amogh," *2015 IEEE Underwater Technology (UT)*, India, pp. 1-9, 2015. [CrossRef] [Google Scholar] [Publisher Link]
- [2] Qi B. Jin, and Q. Liu, "IMC-PID Design Based on Model Matching Approach and Closed-Loop Shaping," *ISA Transactions*, vol. 53, no. 2, pp. 462-473, 2014. [CrossRef] [Google Scholar] [Publisher Link]
- [3] Sukhman Kaur, Sumeet Sagar, and Swati Sondhi, "Internal Model Control Based Fractional Order PID Controller for Knee Joint Motion," *2016 11th International Conference on Industrial and Information Systems (ICIIS)*, India, pp. 318-322, 2016. [CrossRef] [Google Scholar] [Publisher Link]
- [4] Qing Wang, Changhou Lu, and Wei Pan, "IMC PID Controller Tuning for Stable and Unstable Processes with Time Delay," *Chemical Engineering Research and Design*, vol. 105, pp. 120-129, 2016. [CrossRef] [Google Scholar] [Publisher Link]
- [5] Xin-She Yang, "Firefly Algorithm, Stochastic Test Functions and Design Optimisation," *International Journal of Bio-Inspired Computation*, vol. 2, no. 2, pp. 78-84, 2010. [CrossRef] [Google Scholar] [Publisher Link]
- [6] R.A. Krohling, and J.P. Rey, "Design of Optimal Disturbance Rejection PID Controllers Using Genetic Algorithms," *IEEE Transactions on Evolutionary Computation*, vol. 5, no. 1, pp. 78-82, 2001. [CrossRef] [Google Scholar] [Publisher Link]
- [7] Soroush Vahid, and Kaveh Javanmard, "Modeling and Control of Autonomous Underwater Vehicle (AUV) in Heading and Depth Attitude via PPD Controller with State Feedback," *International Journal of Coastal, Offshore and Environmental Engineering*, vol. 1, no. 4, pp. 11-18, 2016. [CrossRef] [Google Scholar] [Publisher Link]
- [8] Dazi Li et al., "Maximum Sensitivity Based Fractional IMC-PID Controller Design for Non-Integer Order System with Time Delay," *Journal of Process Control*, vol. 31, pp. 17-29, 2015. [CrossRef] [Google Scholar] [Publisher Link]

- [9] Bikramaditya Das, Bidyadhar Subudhi, and Bibhuti Bhusan Pati, "Cooperative Formation Control of Autonomous Underwater Vehicles: An Overview," *International Journal of Automation and Computing*, vol. 13, pp. 199-225, 2016. [[CrossRef](#)] [[Google Scholar](#)] [[Publisher Link](#)]
- [10] Sneha D. Joshi, and D.B. Talange, "Integer & Fractional Order PID Controller for Fractional Order Subsystems of AUV," *2013 IEEE Symposium on Industrial Electronics & Applications*, Malaysia, pp. 21-26, 2013. [[CrossRef](#)] [[Google Scholar](#)] [[Publisher Link](#)]
- [11] Mustafa Wassef Hasan, and Nizar Hadi Abbas, "Controller Design for Underwater Robotic Vehicle Based on Improved Whale Optimization Algorithm," *Bulletin of Electrical Engineering and Informatics*, vol. 10, no. 2, pp. 609-618, 2021. [[CrossRef](#)] [[Google Scholar](#)] [[Publisher Link](#)]
- [12] Zhao Zhicheng, Wang Huifang, and Zhang Jinggang, "Design of a Fractional Order PID Controller for High-Order Process with Inverse Response," *Journal of Shanghai Jiaotong University*, vol. 49, no. 8, pp. 1090-1095, 2015. [[Google Scholar](#)] [[Publisher Link](#)]
- [13] Pengchong Chen et al., "Optimal Robust Fractional Order PID Controller Synthesis for First Order Plus Time Delay Systems," *ISA Transactions*, vol. 114, pp. 136-149, 2021. [[CrossRef](#)] [[Google Scholar](#)] [[Publisher Link](#)]